Supplementary Information

Ultrafast charge dynamics of diketopyrrolopyrrole-based terpolymers for optoelectronic applications: impact of acceptor concentrations and thermal annealing

Leonato Tambua Nchinda,*[a] Zewdneh Genene,[b] Wendimagegn Mammo,[c] Newayemedhin A. Tegegne,[d] Dirk M. Guldi,[e] Tjaart P. J. Krüger[a,f]

[a]*Department of Physics, University of Pretoria, Private Bag X20, Hatfield 0028, South Africa.*

[b]*Department of Chemistry and Chemical Engineering, Chalmers University of Technology, SE412 96, Gothenburg, Sweden.*

[c]*Department of Chemistry, Addis Ababa University, 33658, Addis Ababa, Ethiopia.*

[d]*Department of Physics, Addis Ababa University, Addis Ababa, 1176, Ethiopia.*

[e]*Department of Chemistry and Pharmacy & Interdisciplinary Center for Molecular Materials (ICMM), FAU Profile Center Solar, Friedrich-Alexander-Universität Erlangen-Nürnberg, Erlangen, Germany.*

[f]*National Institute for Theoretical and Computational Sciences (NITheCS), South Africa.*

*Corresponding author: leonato.nchinda@tuks.co.za

Table S1 Photovoltaic parameters and properties of **P1**–**P3**:$PC_{71}BM$ organic solar cells[1] The average and standard deviation values were calculated from 8 devices. μ_h and μ_e represent the hole and electron mobilities.

Parameters	**P1**:$PC_{71}BM$	**P2**:$PC_{71}BM$	**P3**:$PC_{71}BM$
V_{oc} [V]	0.62 ± 0.01	0.64 ± 0.01	0.66 ± 0.01
J_{sc} [$mAcm^{-2}$]	15.20 ± 0.37	8.24 ± 0.08	10.40 ± 0.17
FF	0.60 ± 0.01	0.59 ± 0.01	0.52 ± 0.01
PCE [%]	5.58 ± 0.09	3.10 ± 0.08	3.57 ± 0.07
μ_h[$cm^2V^{-1}s^{-1}$]	5.98×10^{-4}	3.71×10^{-4}	3.25×10^{-4}
μ_e[$cm^2V^{-1}s^{-1}$]	2.83×10^{-4}	2.10×10^{-4}	1.78×10^{-4}
μ_h/μ_e	2.1	1.8	1.8

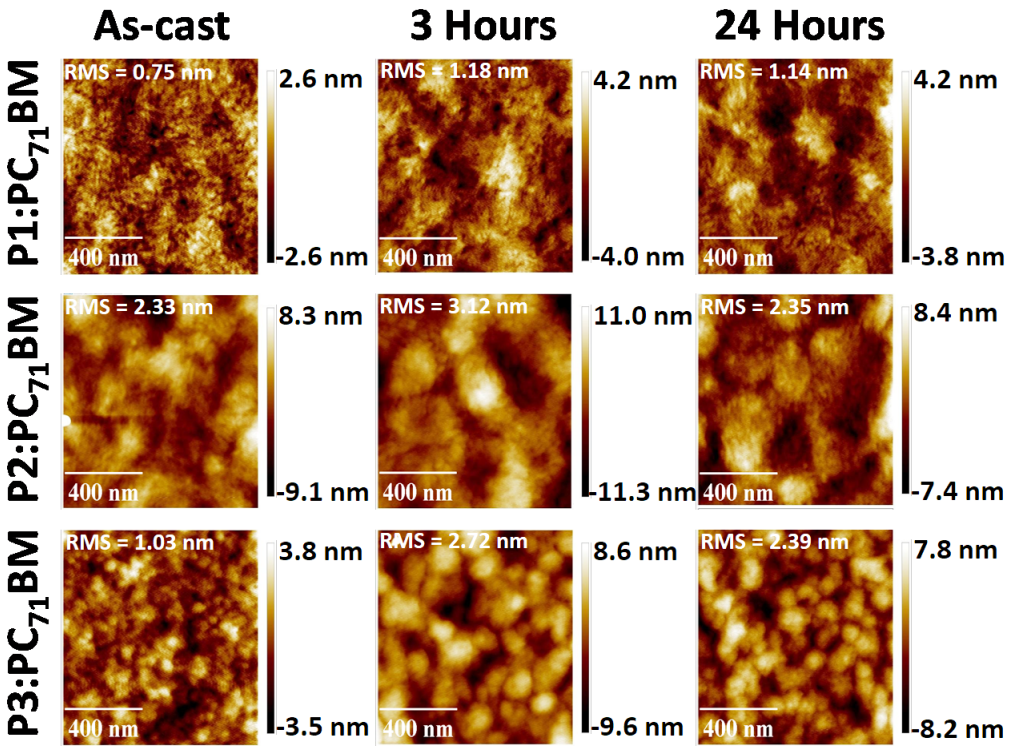

Figure S1 Atomic force microscopy images ($1 \times 1\ \mu m^2$) of **P1**–**P3**:$PC_{71}BM$ thin films showing their root mean square surface roughness prior to thermal annealing (left) and after thermal degradation at 85 °C for 3 h (middle) and 24 h (right).[2]

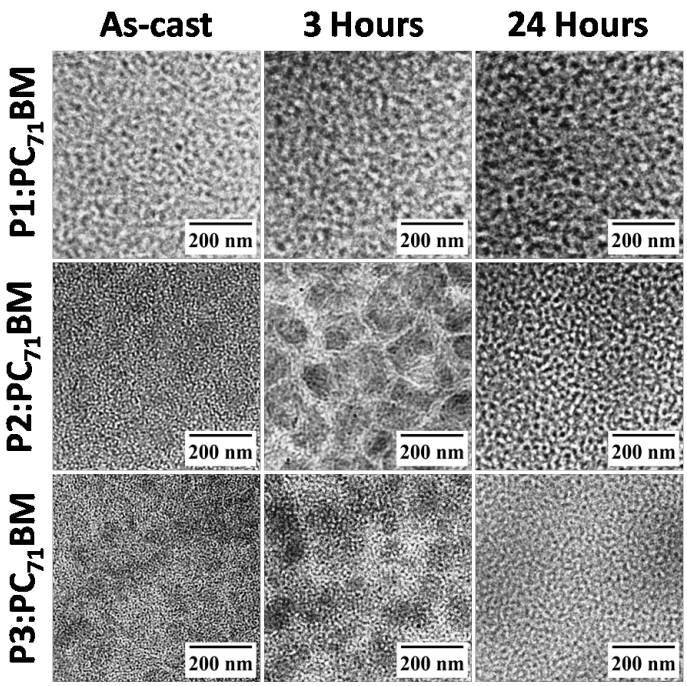

Figure S2 TEM images of **P1**–**P3**:$PC_{71}BM$ thin films showing the as-cast (left) and thermally annealed thin films at 85 °C for 3 hours (middle) and 24 hours (right).[2]

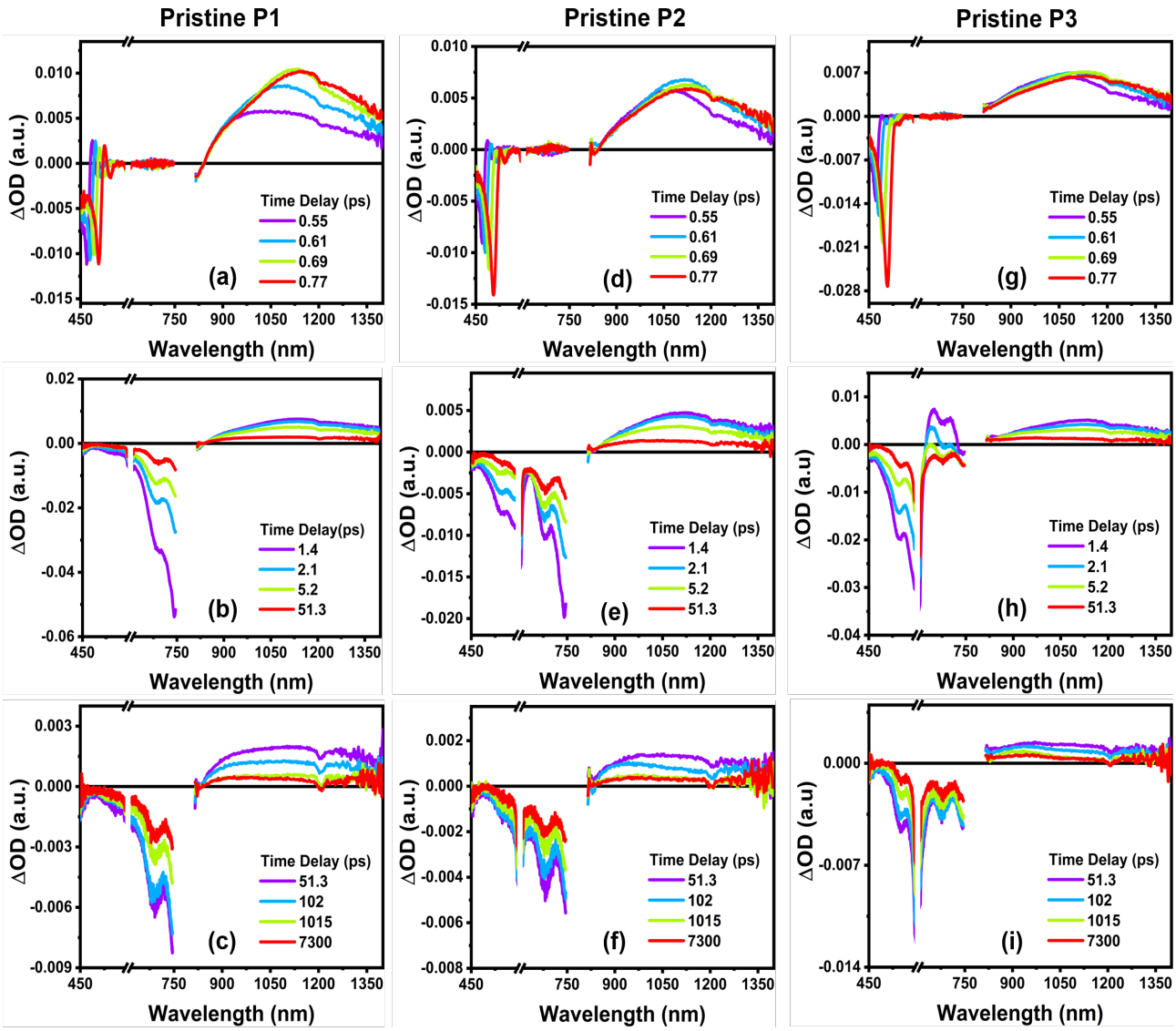

Figure S3 TA spectra of as-cast pristine (a-c) **P1** (d-f) **P2** and (g-i) **P3** thin films excited at 600 nm at 0.5 μJ/pulse·cm^2. Each panel presents the TA results corresponding to different delay time ranges.

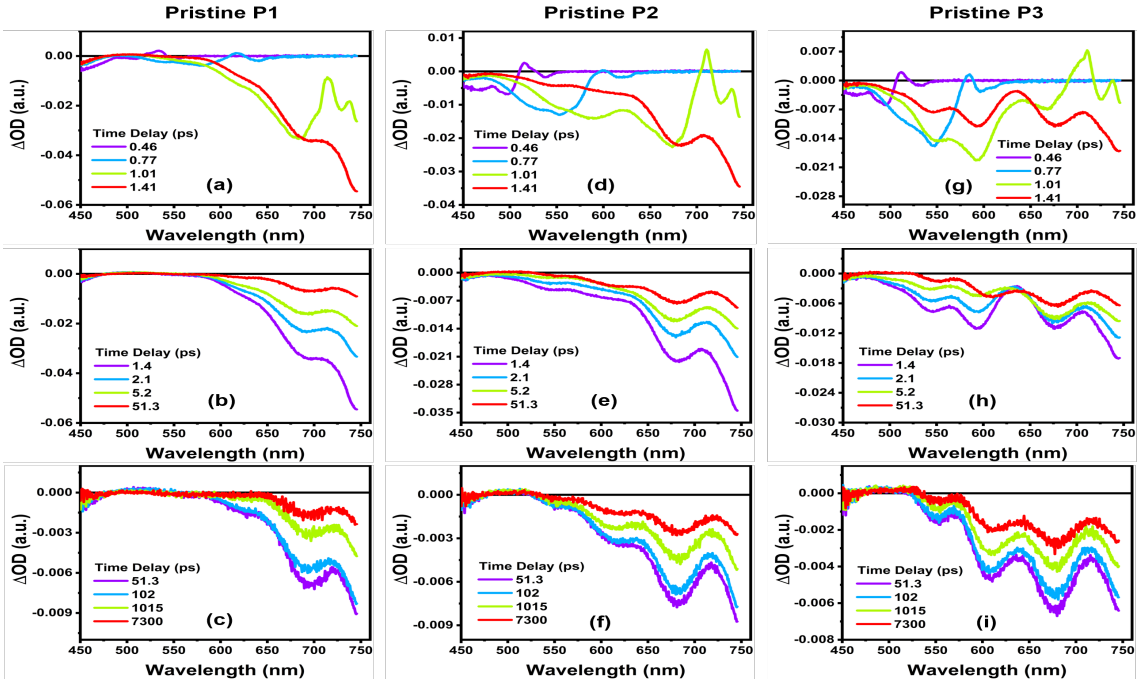

Figure S4 TA spectra of as-cast pristine (a-c) **P1** (d-f) **P2** and (g-i) **P3** thin films excited at 800 nm at 1.0 μJ/pulse·cm^2 and probed in the visible region. Each panel presents the TA results corresponding to different delay time ranges.

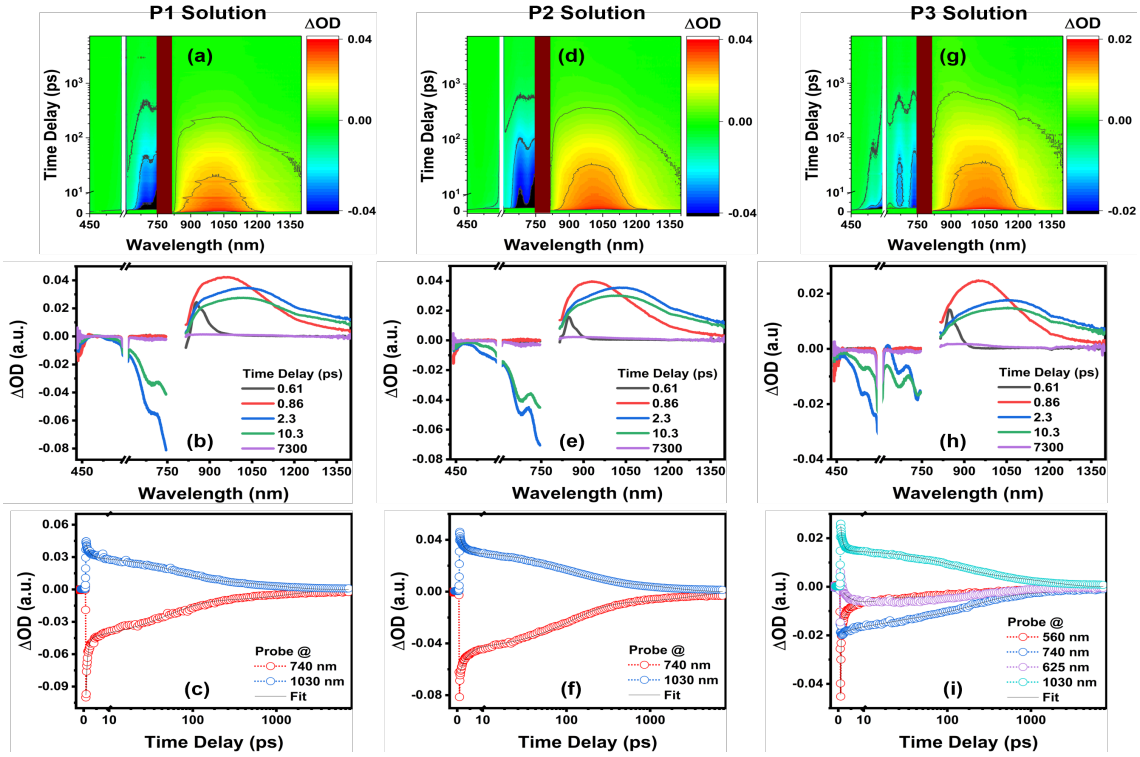

Figure S5 2D color plots (a, d, and g) and TA spectra of pristine (a and b) **P1** (d and e) **P2**, and (g and h) **P3** terpolymers in DCB solution excited at 600 nm at 0.4 μJ/pulse·cm^2. TA traces probed at different wavelengths from the pristine (c) **P1** (f) **P2** and (i) **P3** solutions pumped at 600 nm.

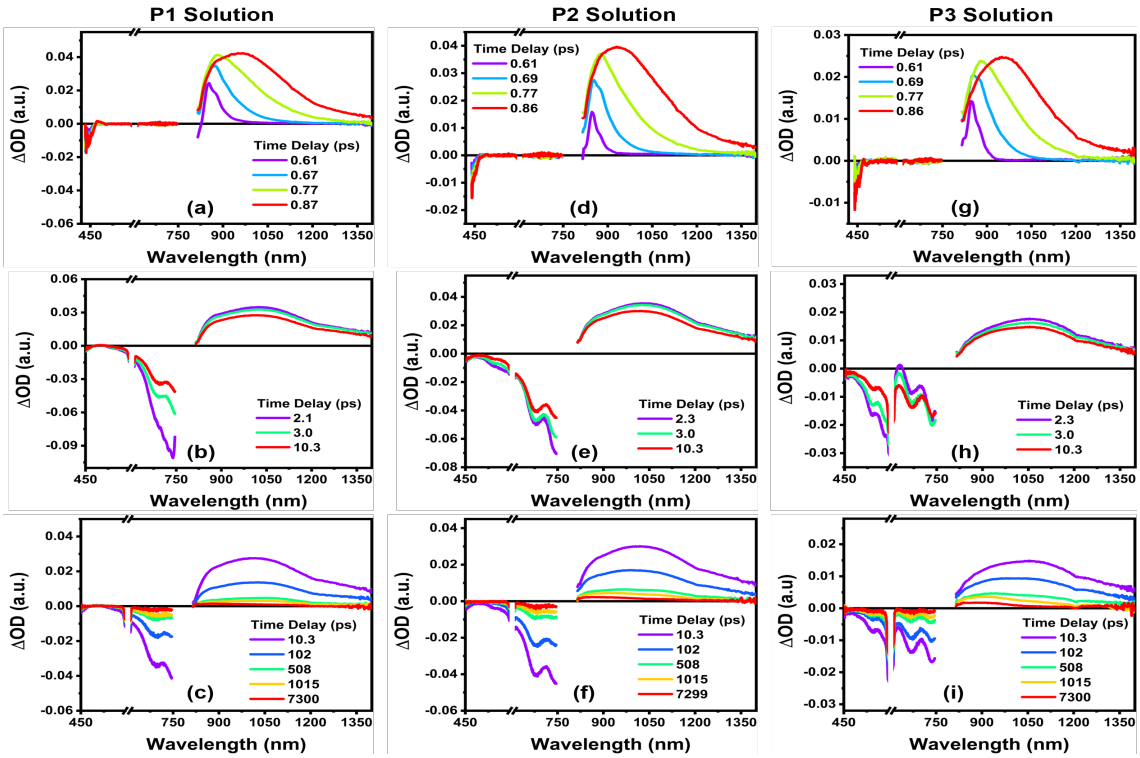

Figure S6 TA spectra of pristine (a-c) **P1** (d-f) **P2** and (g-i) **P3** terpolymers in DCB solution pumped at 600 nm at 0.4 μJ/pulse·cm^2. Each panel presents the TA results corresponding to different delay time ranges.

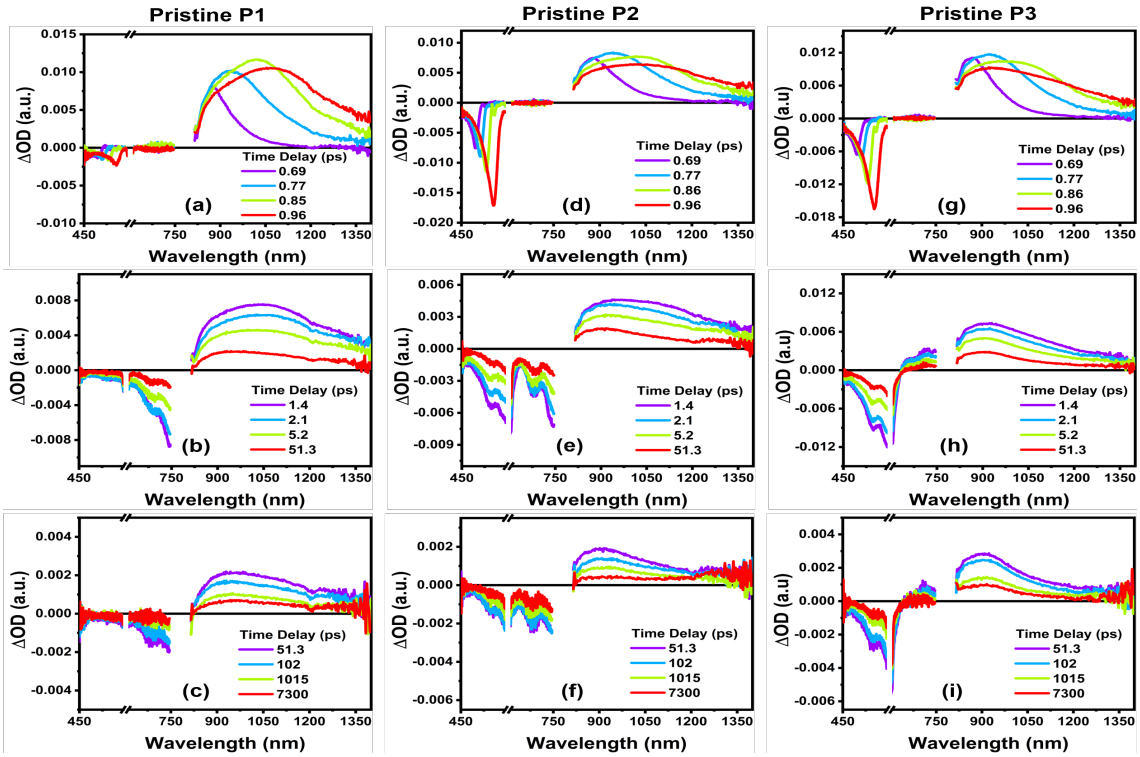

Figure S7 TA spectra of pristine (a-c) **P1** (d-f) **P2** and (g-i) **P3** thin films thermally degraded for 24 h and excited at 600 nm at 0.5 μJ/pulse·cm^2. Each panel presents the TA results corresponding to different delay time ranges.

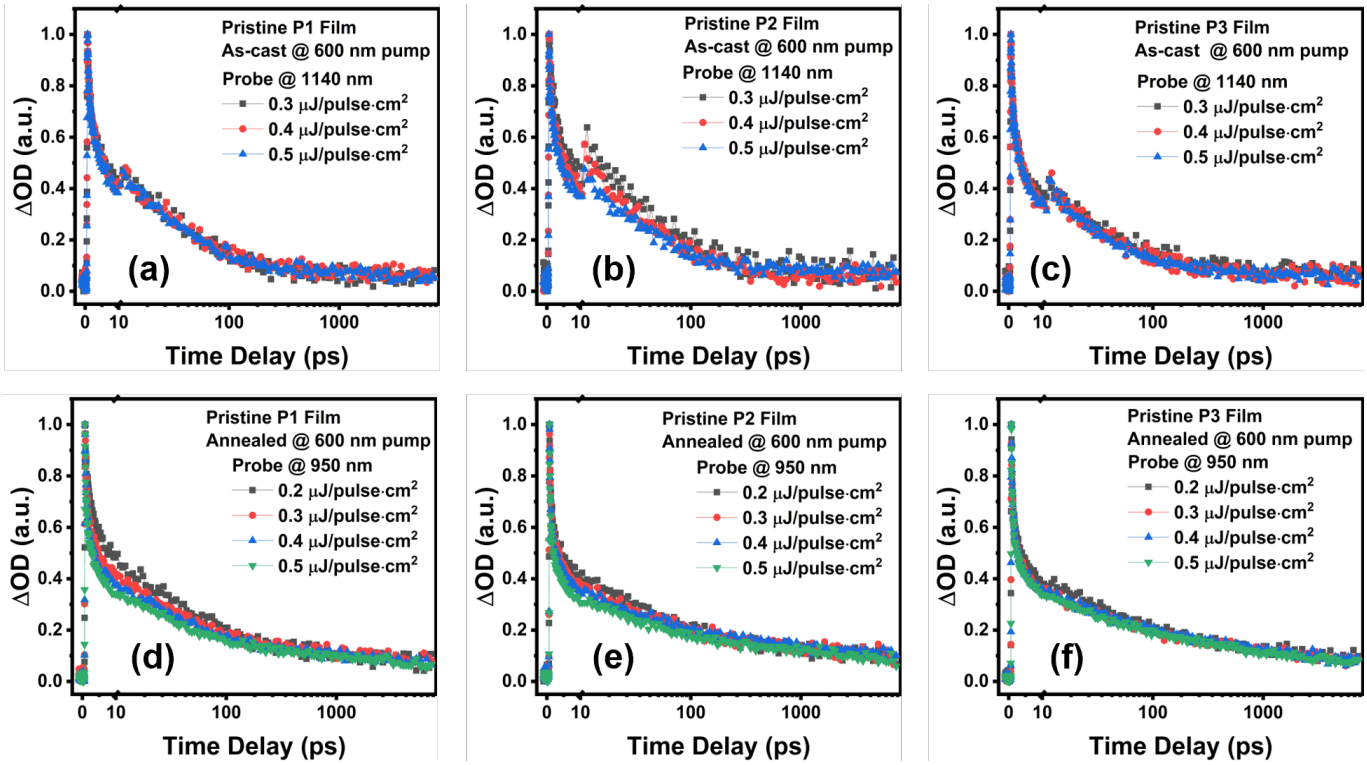

Figure S8 Pump-fluence-dependence of ESA decay profiles of as-cast (a-c) and degraded (d-f) pristine **P1** (a,d), **P2** (b,e), and **P3** (c,f) thin films at 600 nm excitation.

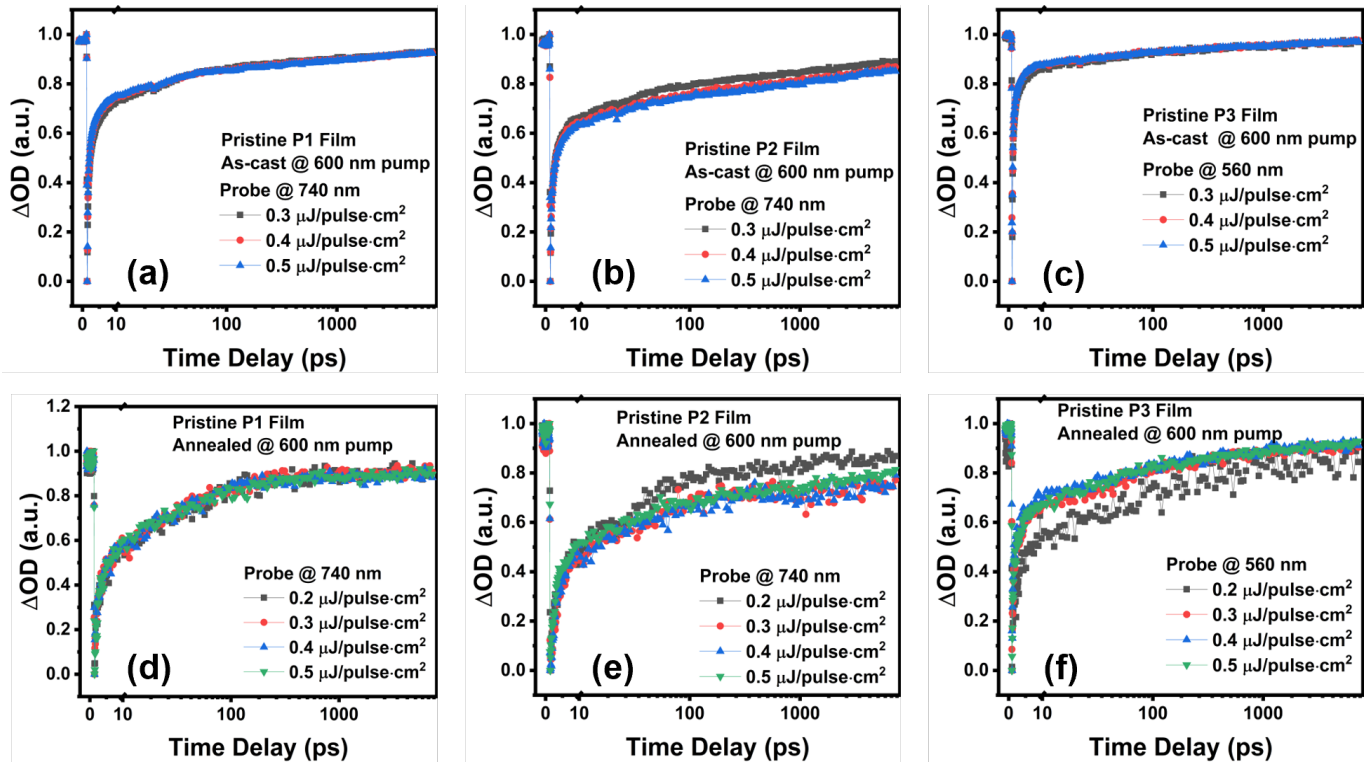

Figure S9 Pump-fluence-dependence of GSB decay profiles of as-cast (a-c) and degraded (d-f) pristine **P1** (a,d), **P2** (b,e), and **P3** (c,f) thin films at 600 nm excitation.

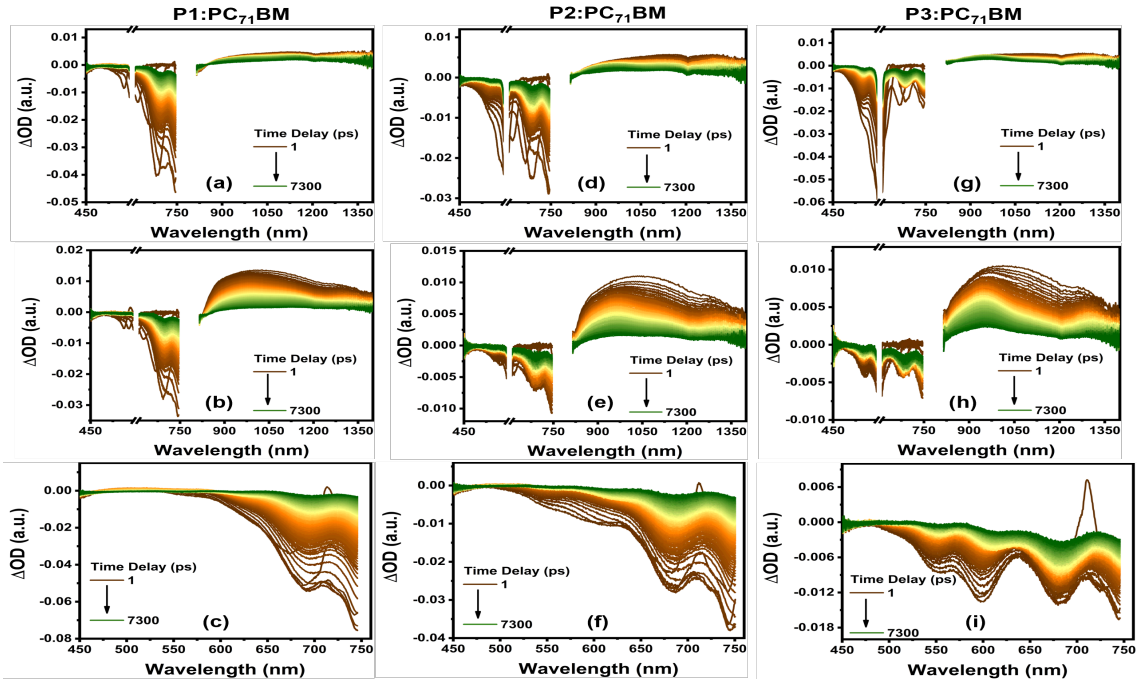

Figure S10 TA spectra of as-cast (a) **P1**:$PC_{71}BM$ (d) **P2**:$PC_{71}BM$ and (g) **P3**:$PC_{71}BM$ and thermally degraded (b) **P1**:$PC_{71}BM$ (e) **P2**:$PC_{71}BM$ and (h) **P3**:$PC_{71}BM$ thin films pumped at 600 nm at 0.5 μJ/pulse·cm^2. TA spectra of as-cast (c) **P1**:$PC_{71}BM$ (f) **P2**:$PC_{71}BM$ and (i) **P3**:$PC_{71}BM$ blend films pumped at 800 nm at 1.0 μJ/pulse·cm^2 and probed in the visible region.

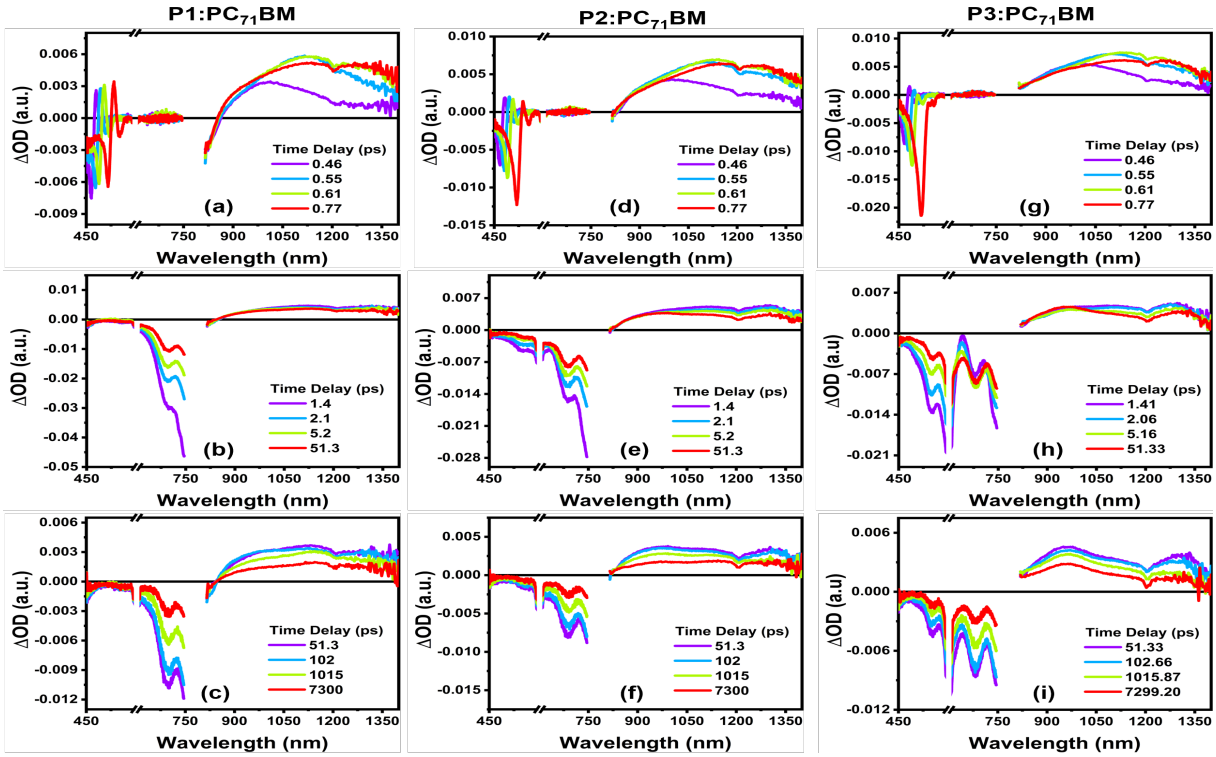

Figure S11 TA spectra of as-cast (a-c) **P1**:$PC_{71}BM$ (d-f) **P2**:$PC_{71}BM$ and (g-i) **P3**:$PC_{71}BM$ blend films excited at 600 nm at 0.5 μJ/pulse·cm^2. Each panel presents the TA results corresponding to different delay time ranges.

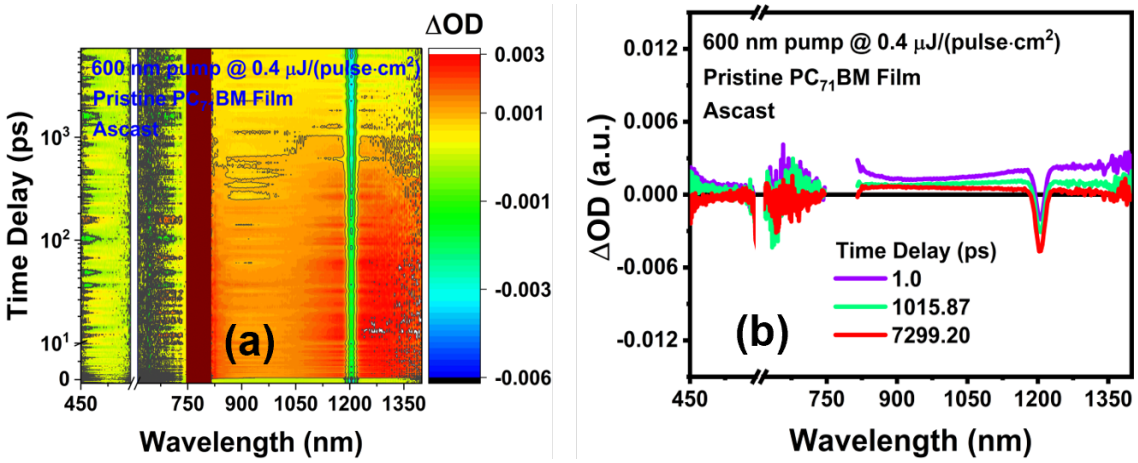

Figure S12 TA spectra of pristine $PC_{71}BM$ thin film excited at 600 nm.

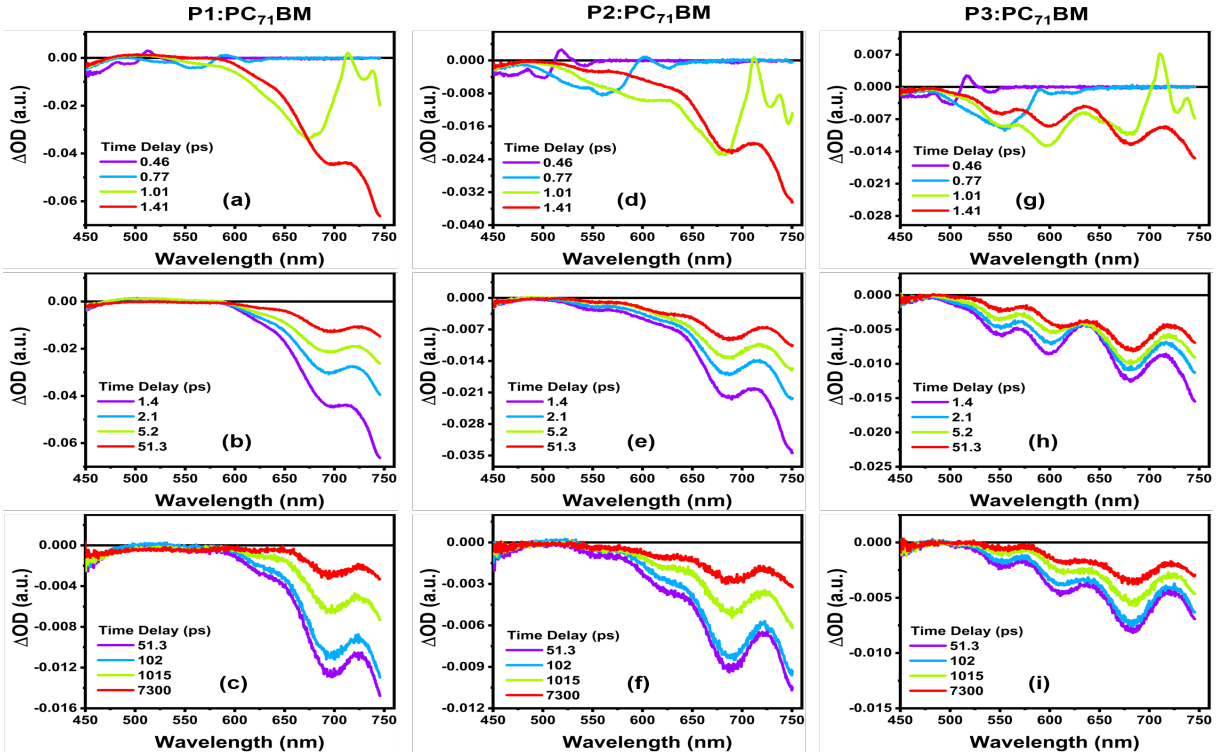

Figure S13 TA spectra of as-cast (a-c) **P1**:$PC_{71}BM$ (d-f) **P2**:$PC_{71}BM$ and (g-i) **P3**:$PC_{71}BM$ blend films excited at 800 nm at 1.0 μJ/pulse·cm^2 and probed in the visible region. Each panel presents the TA results corresponding to different delay time ranges.

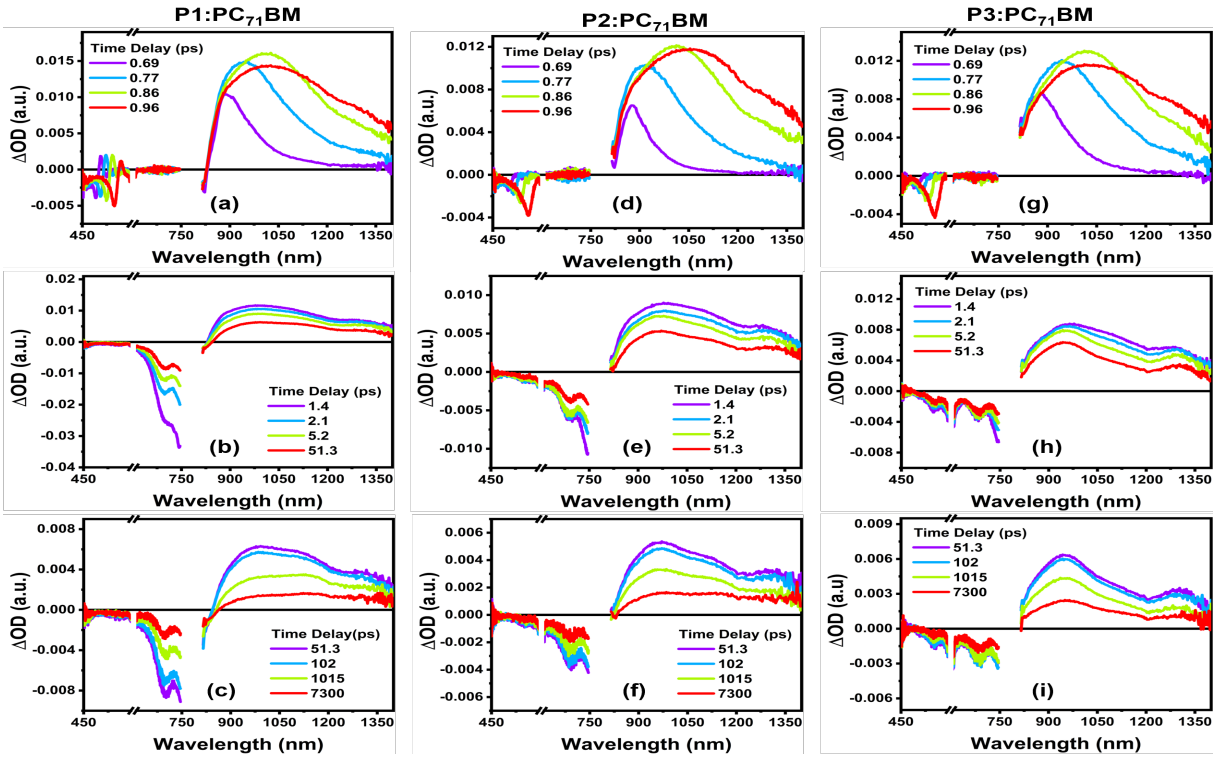

Figure S14 TA spectra of (a-c) **P1**:$PC_{71}BM$ (d-f) **P2**:$PC_{71}BM$ and (g-i) **P3**:$PC_{71}BM$ blend films thermally degraded for 24 h and excited at 600 nm at 0.5 μJ/pulse·cm^2. Each panel presents the TA results corresponding to different delay time ranges.

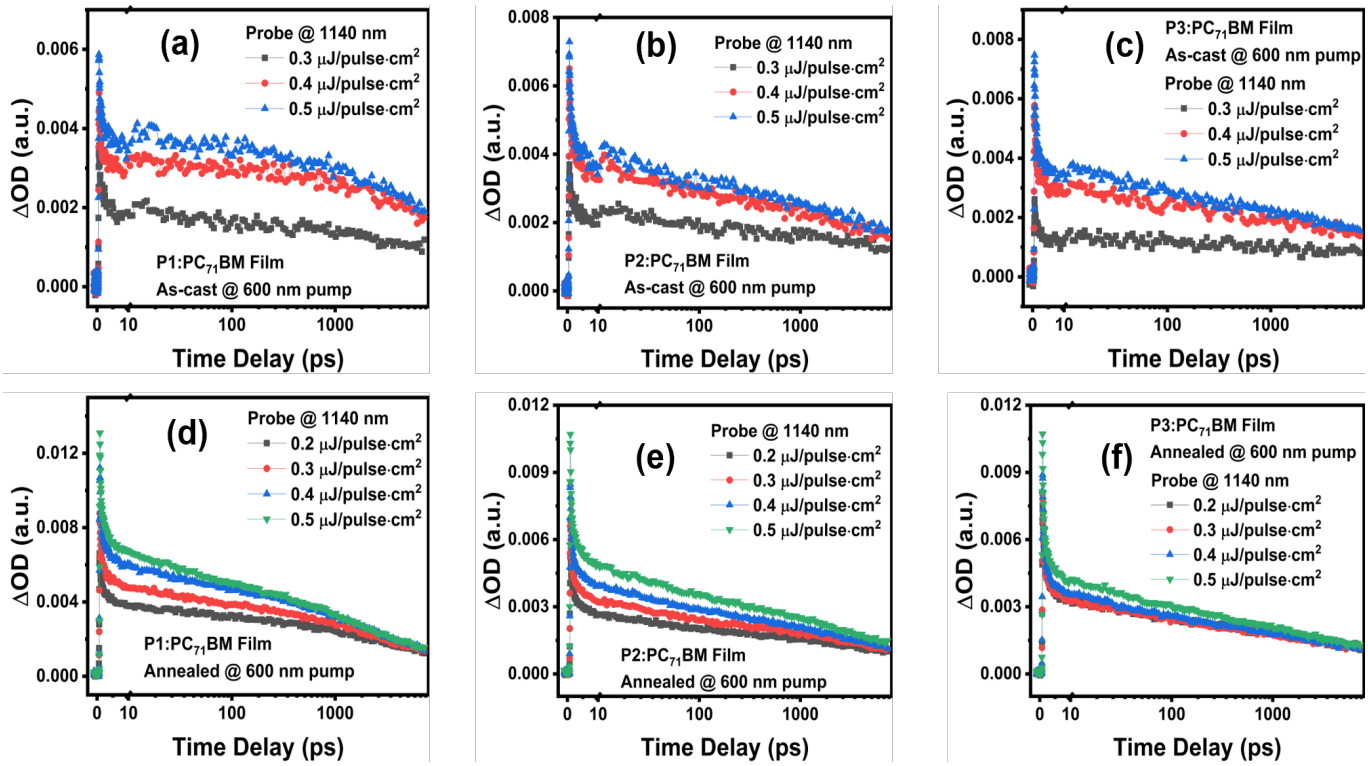

Figure S15 Pump-fluence-dependence of ESA decay profiles at 1140 nm for as-cast (a-c) and degraded (d-f) blends of **P1** (a,d), **P2** (b,e), and **P3** (c,f) thin films at 600 nm excitation.

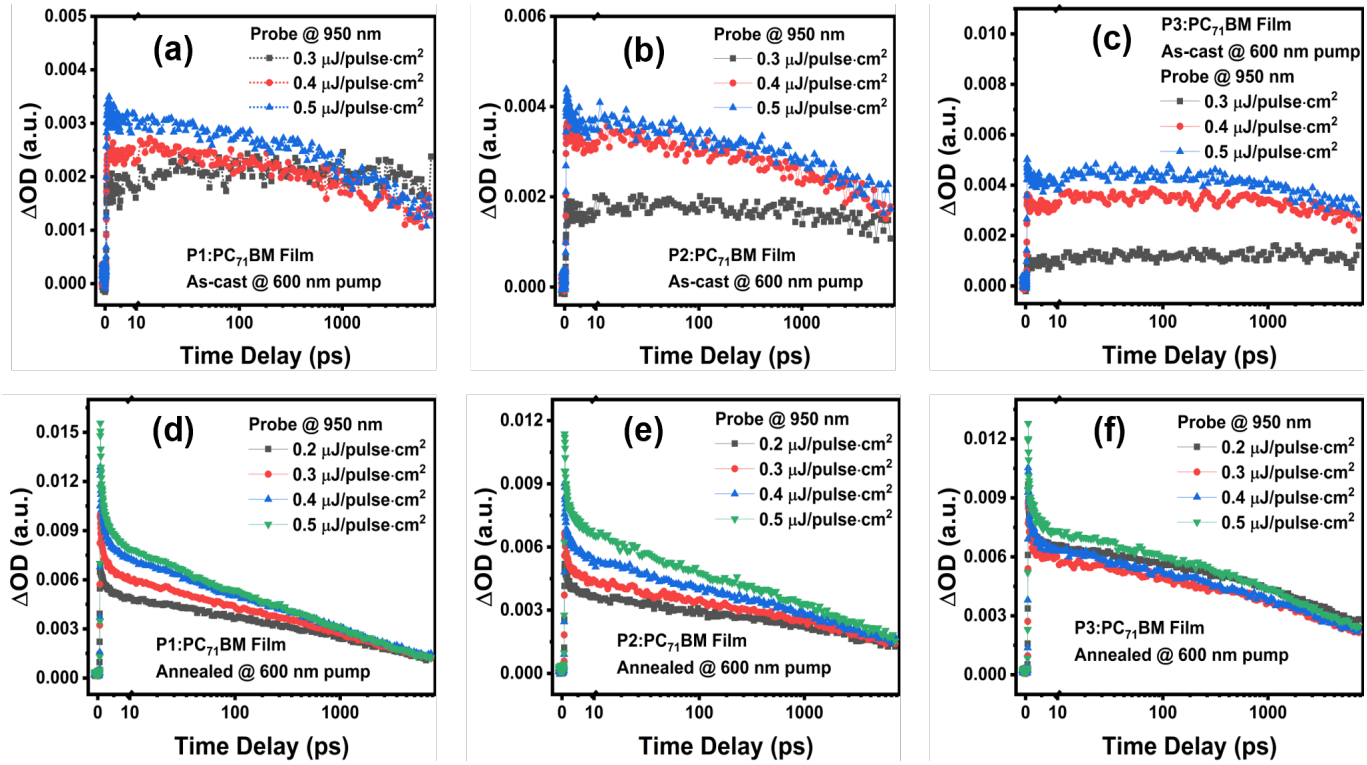

Figure S16 Pump-fluence-dependent TA traces probed at 950 nm for as-cast (a-c) and thermally degraded (d-f) blends of **P1** (a,d), **P2** (b,e), and **P3** (c,f) thin films at 600 nm excitation. The fluence dependence of decay dynamics is characteristic behavior for bimolecular recombination of free polarons for the CT state.

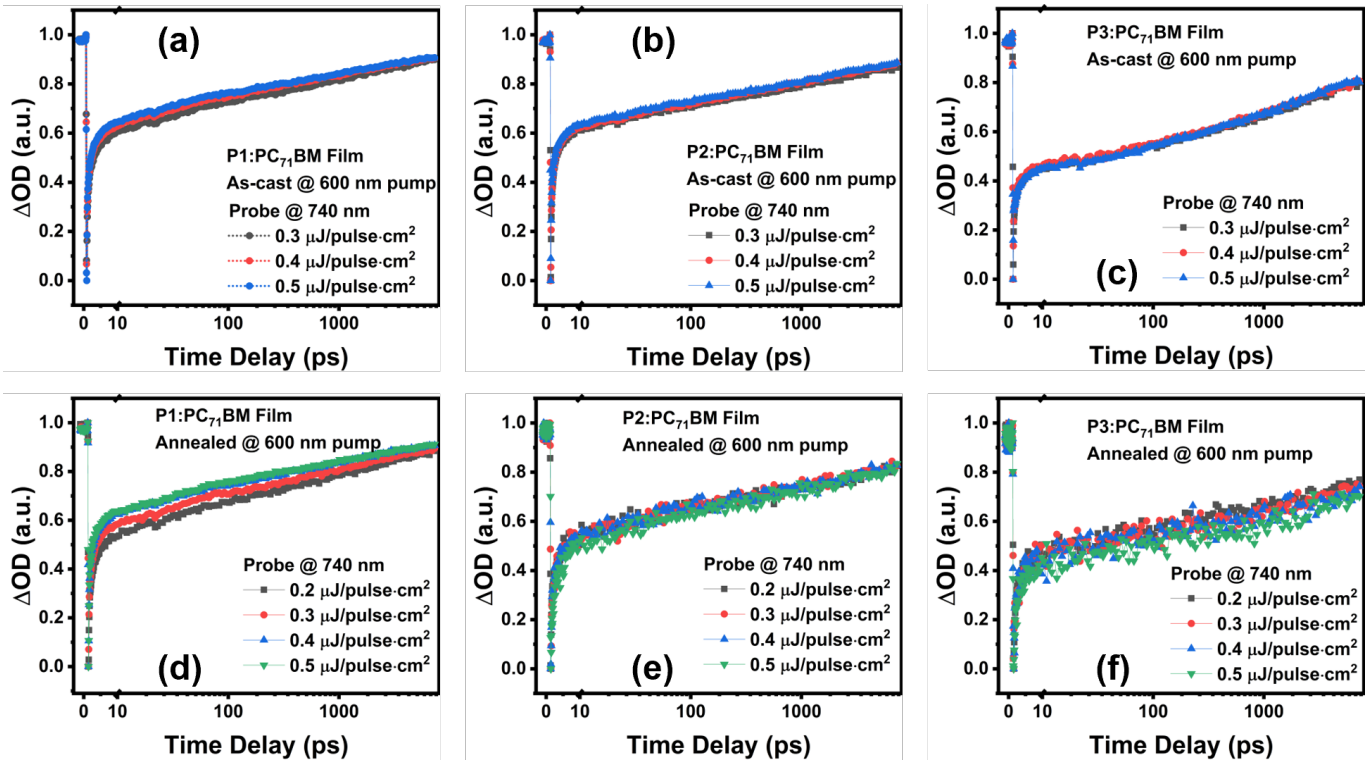

Figure S17 Pump-fluence-dependent TA traces probed at 740 nm for as-cast (a-c) and thermally degraded (d-f) blends of **P1** (a,d), **P2** (b,e), and **P3** (c,f) thin films at 600 nm excitation.

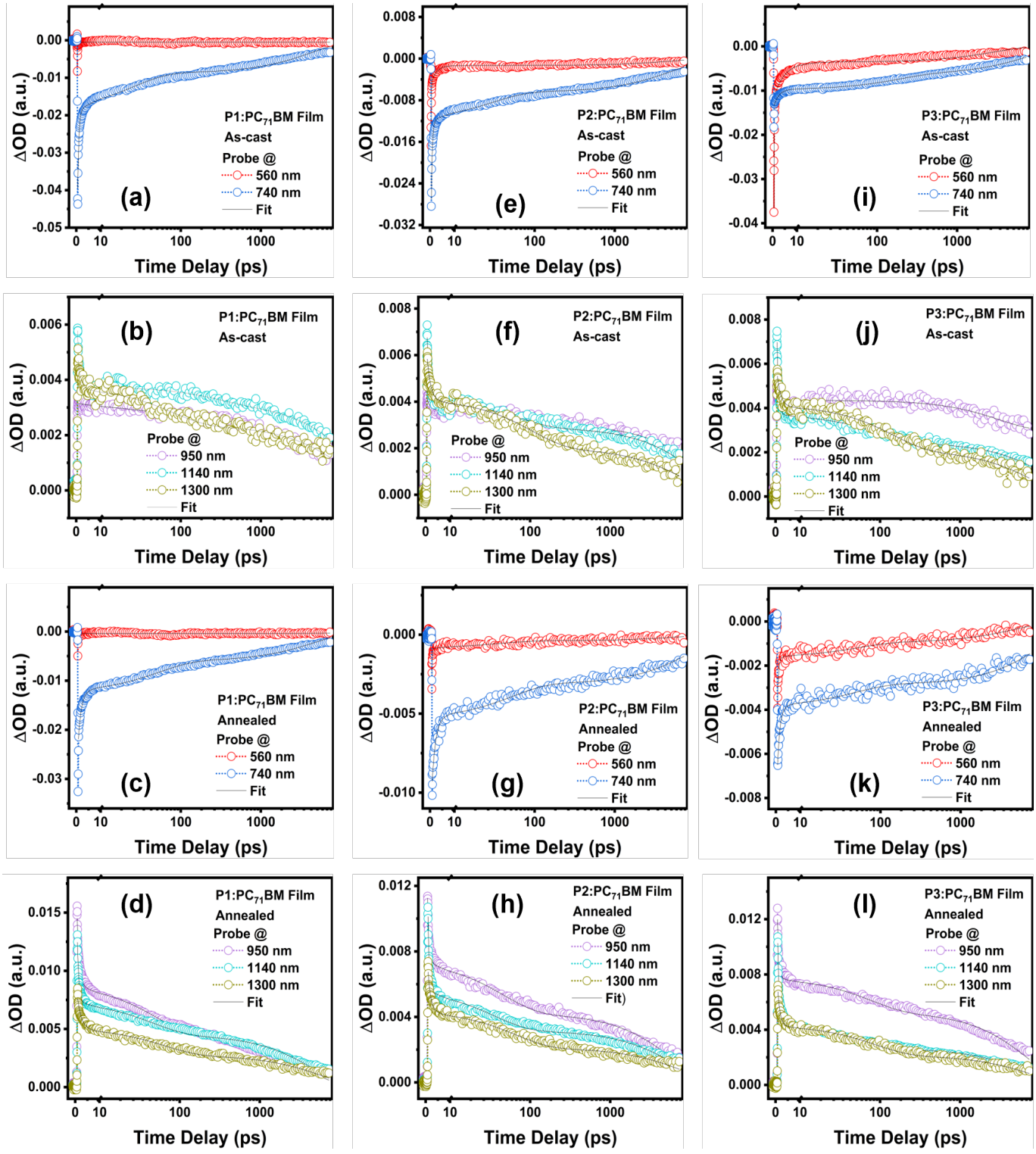

Figure S18 Kinetic traces of as-cast: (a,b) **P1**:$PC_{71}BM$ (e,f) **P2**:$PC_{71}BM$ and (i,j) **P3**:$PC_{71}BM$ and degraded: (c,d) **P1**:$PC_{71}BM$ (g,h) **P2**:$PC_{71}BM$ and (k,l) **P3**:$PC_{71}BM$ blend films pumped at 600 nm at 0.5 μJ/pulse·cm^2.

Table S2 Time constants from fitting on the TA decay profiles with multi-exponential function, $I = A_1 e^{\frac{-t}{\tau_1}} + A_2 e^{\frac{-t}{\tau_2}} + A_3 e^{\frac{-t}{\tau_3}}$. A is normalized amplitude in percentage where $A = \frac{A_i}{(A_1+A_2+A_3)} \times 100$.

Sample	λ (nm)	τ_1 (ps)	A_1 (%)	τ_2 (ps)	A_2 (%)	τ_3 (ps)	A_3 (%)
P1 Solution	740	0.67	96.03	50.1	3.03	1628	0.94
	1030	1.2	43.85	67.5	40.19	1025	15.96
P2 Solution	740	2.8	47.40	114.8	41.53	3417	11.07
	1030	1.4	42.97	106.1	41.81	1673	15.22
P3 Solution	560	0.16	99.99	4.2	-	613.8	-
	740	13.3	27.62	216.6	55.28	4034	17.10
	1030	0.82	67.56	121.7	20.80	1584	11.64
P1 Film As-cast	560	0.12	99.98	1.3	0.02	>7300	-
	740	0.45	97.43	15.7	1.76	5184	0.81
	1140	1.2	60.65	36.9	33.57	4257	5.78
P1 Film Deg	560	0.19	99.3	3.9	0.60	1507	0.15
	740	1.7	70.55	37.1	22.78	>7300	6.67
	950	0.64	77.66	25.1	16.07	5639	6.27
P2 Film As-cast	560	0.14	99.95	2.1	0.04	2911	0.01
	740	0.80	86.64	25.1	6.94	>7300	6.41
	1140	1.3	60.52	40.7	33.87	>7300	5.61
P2 Film Deg	560	0.17	99.82	4.7	0.14	2577	0.04
	740	1.7	63.24	33.5	18.43	>7300	18.33
	950	0.58	81.67	24.6	11.91	6701	6.42
	1140	0.66	81.49	20.1	14.25	5555	4.26
P3 Film As-cast	560	0.19	99.77	3.9	0.18	2175	0.05
	645	0.12	99.97	1.1	0.01	1.1	0.02
	740	187.6	1.82	1671	27.80	>7300	70.3
	1140	1.1	65.13	33.8	29.76	6885	5.11
P3 Film Deg	560	0.58	86.77	26.2	9.02	5046	4.21
	740	0.09	99.99	3.9	-	115.8	-
	950	0.60	79.76	26.2	13.09	5187	7.16
	1140	0.42	91.96	14.1	6.02	2353	2.02
P1:$PC_{71}BM$ Film As-cast	560	0.08	99.99	0.83	-	>7300	-
	740	0.48	95.27	25.0	2.59	4373	2.14
	950	24.3	10.20	1006	27.70	>7300	62.00
	1140	0.66	56.70	278.6	6.91	>7300	36.40
	1300	1.2	33.03	76.9	24.78	>7300	42.19
P1:$PC_{71}BM$ Film Deg	560	0.10	99.99	0.84	0.01	>7300	-
	740	1.2	72.80	52.2	14.07	4736	13.13
	950	0.88	61.73	50.4	18.96	3636	19.31
	1140	0.62	74.81	45.1	9.90	4509	15.29
	1300	1.6	47.91	62.5	24.21	5829	27.87
P2:$PC_{71}BM$ Film As-cast	560	0.10	99.99	2.1	0.01	4942	-
	740	0.45	96.10	29.3	1.83	5270	2.07
	950	1.3	17.50	197.3	14.30	>7300	68.20
	1140	0.77	60.29	70.7	11.65	>7300	28.06

	1300	1.4	40.55	103.9	30.45	>7300	29.0
P2:$PC_{71}BM$ Film Deg	560	0.17	99.90	34.5	0.07	6239	0.06
	740	1.4	65.90	51.9	14.22	>7300	19.87
	950	0.63	65.55	45.3	14.86	5708	19.59
	1140	0.51	83.54	35.2	7.32	6295	9.14
	1300	1.2	56.66	64.6	22.61	>7300	20.73
P3:$PC_{71}BM$ Film As-cast	560	0.15	99.89	4.4	0.08	2816	0.03
	740	2.1	42.34	180.8	20.26	>7300	37.40
	950	3057	31.95	>7300	34.02	>7300	34.02
	1140	0.62	70.10	92.4	10.37	>7300	19.53
	1300	1.4	35.67	140.9	31.78	>7300	32.55
P3:$PC_{71}BM$ Film Deg	560	0.44	92.26	52.6	3.22	4835	4.52
	740	1.1	72.42	48.1	7.36	>7300	20.23
	950	0.56	69.90	75.2	9.58	6958	20.52
	1140	0.53	86.09	38.1	6.37	6726	7.54
	1300	0.99	59.36	86.1	20.51	>7300	20.13
Sample	λ (nm)	τ_1 (ps)	A_1 (%)	τ_2 (ps)	A_2 (%)	τ_3 (ps)	A_3 (%)

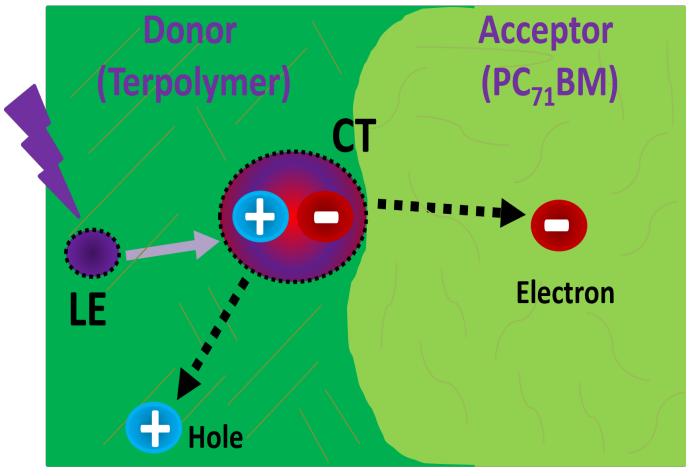

Figure S19 Donor-acceptor interface in OSCs and a simplified representation of their operational mechanism.

References

[1] A. Negash, Z. Genene, R. T. Eachambadi, J. Kesters, N. V. d. Brande, J. D'Haen, H. Penxten, B. Abdulahi, E. Wang, K. Vandewal, W. Maes, W. Mammo, J. Manca and S. Admassie, *J. Mater. Chem. C*, 2019, **7**, 3375–3384.

[2] L. T. Nchinda, Z. Genene, W. Mammo, N. A. Tegegne and T. P. J. Krüger, *New J. Chem.*, 2024, **48**, 10201–10212.